Enhancing zinc-finger-nuclease activity with improved obligate heterodimeric architectures

Yannick Doyon, Thuy D Vo, Matthew C Mendel, Shon G Greenberg, Jianbin Wang, Danny F Xia, Jeffrey C Miller, Fyodor D Urnov, Philip D Gregory & Michael C Holmes

Zinc-finger nucleases (ZFNs) drive efficient genome editing by introducing a double-strand break into the targeted gene. Cleavage is induced when two custom-designed ZFNs heterodimerize upon binding DNA to form a catalytically active nuclease complex. The importance of this dimerization event for subsequent cleavage activity has stimulated efforts to engineer the nuclease interface to prevent undesired homodimerization. Here we report the development and application of a yeast-based selection system designed to functionally interrogate the ZFN dimer interface. We identified critical residues involved in dimerization through the isolation of cold-sensitive nuclease domains. We used these residues to engineer ZFNs that have superior cleavage activity while suppressing homodimerization. The improvements were portable to orthogonal domains, allowing the concomitant and independent cleavage of two loci using two different ZFN pairs. These ZFN architectures provide a general means for obtaining highly efficient and specific genome modification.

Zinc-finger nucleases (ZFNs) are hybrid restriction enzymes composed of a customizable zinc-finger protein DNA-binding domain fused to the cleavage domain of the FokI endonuclease[1]. As the zinc-finger protein DNA-binding domain can be engineered to bind with high specificity to an investigator's chosen sequence[2], ZFNs enable a DNA cleavage event to be targeted to effectively any genomic location. Subsequent repair of the ZFN-induced double-strand break by the evolutionarily conserved non-homologous end-joining or homology-directed repair pathways facilitates the precise modification of the targeted endogenous gene. ZFN-driven 'genome editing' has been demonstrated in a broad range of species, including those for which facile reverse genetics was not available previously, and has been a highly efficient tool for making precise genomic modifications in transformed and primary human cells[3,4].

Given the broad potential utility of ZFNs in genome engineering, considerable effort has been directed to methods that increase the cleavage activity and/or specificity of ZFNs. Three major determinants have been examined to date; the zinc-finger protein DNA-binding domain[5], the FokI nuclease domain[6,7] and the linker sequence connecting the two[8]. Although optimization of the DNA-binding domain can improve a specific ZFN pair[9], the modularity of the FokI domain offers the potential for improvements to be portable to all ZFNs. To this end, we and others previously used structure-guided design to develop modified FokI domains that function as obligate heterodimers[6,7] and thus increase specificity. However, the mutations originally described also exhibited a reduction in dimerization energy revealed as a reduced rate of cutting *in vitro*[6] and *in vivo*[6,10]. As FokI dimerization is necessary for DNA cleavage[11] the residues important for dimer formation remain attractive targets for development of ZFN architectures with improved specificity and activity.

Here we exploit a yeast-based selection system to interrogate the dimer interface. We adapted a reporter assay, previously developed for the identification of active nucleases from a panel of preassembled ZFNs[12–15], for the isolation of mutations in the FokI domain conferring cold-sensitivity. We reasoned that the isolation of cold-sensitive mutants could pinpoint critical residues involved in dimerization because this class of mutations is often associated with defects in assembly of multisubunit protein complexes[16]. We report the identification of such mutations and their use to guide the rational design of new FokI domains that have superior cleavage activity and retain obligate heterodimer function. The engineered substitutions also increased the activity of recently described orthogonal FokI domains[10], improving the efficiency and specificity with which independent loci can be concomitantly targeted using two ZFNs. These enhanced FokI domains were portable to many zinc-finger proteins, independent of cell type, and are a general solution for improved ZFN activity.

RESULTS

Isolation of cold-sensitive FokI mutants

We developed a selection system in *Saccharomyces cerevisiae* to isolate ZFN mutants displaying a cold-sensitivity phenotype, that is, cleavage activity that is severely diminished at lower temperatures but robust at higher ones. The system uses two independent single-strand annealing reporter constructs integrated into the yeast genome that contain a binding site for the *CCR5-L* ZFN homodimer[17] (**Fig. 1a**). For both reporters, a ZFN-induced

Sangamo BioSciences, Richmond, California, USA. Correspondence should be addressed to Y.D. (ydoyon@sangamo.com).

RECEIVED 4 JUNE; ACCEPTED 5 NOVEMBER; PUBLISHED ONLINE 5 DECEMBER 2010; DOI:10.1038/NMETH.1539

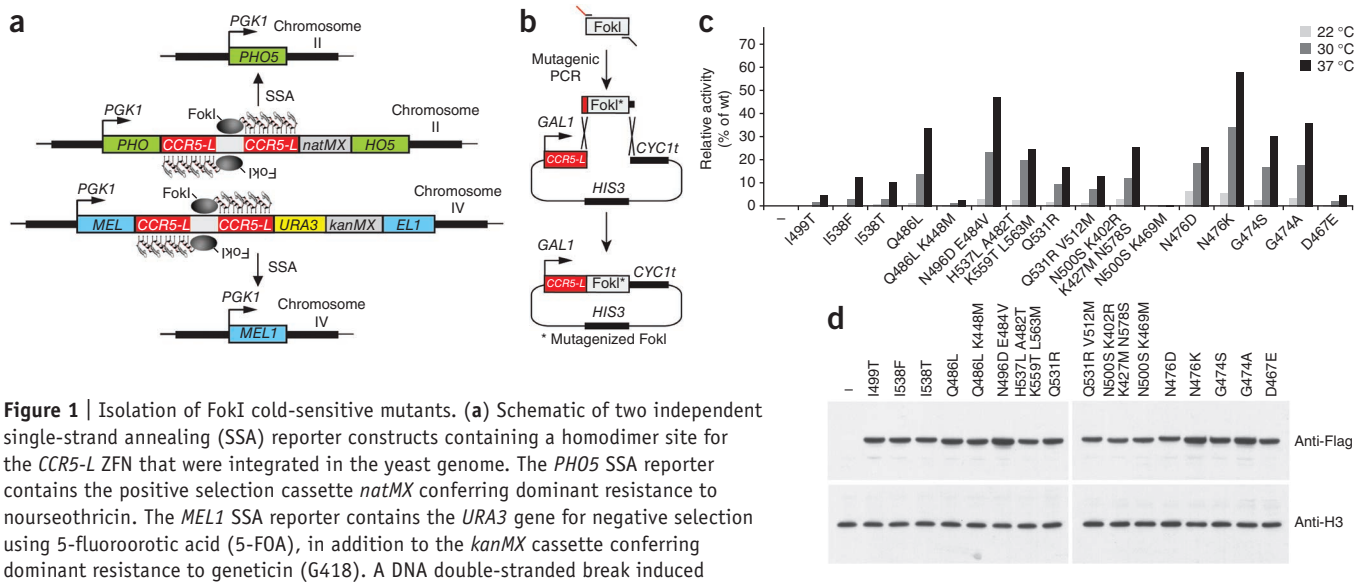

Figure 1 | Isolation of FokI cold-sensitive mutants. (**a**) Schematic of two independent single-strand annealing (SSA) reporter constructs containing a homodimer site for the *CCR5-L* ZFN that were integrated in the yeast genome. The *PHO5* SSA reporter contains the positive selection cassette *natMX* conferring dominant resistance to nourseothricin. The *MEL1* SSA reporter contains the *URA3* gene for negative selection using 5-fluoroorotic acid (5-FOA), in addition to the *kanMX* cassette conferring dominant resistance to geneticin (G418). A DNA double-stranded break induced by a functional homodimeric ZFN will result in reconstitution of the reporter genes and elimination of both positive and negative selection markers. *PHO*, 5′ fragment of *PHO5*; *HO5*, 3′ fragment of *PHO5*; *MEL*, 5′ fragment of *MEL1*; and *EL1*, 3′ fragment of *MEL1*. (**b**) Schematic depicting random mutagenesis of the FokI nuclease domain and assembly of the library of mutants. *CYC1t*, transcription terminator of the *CYC1* gene. *S. cerevisiae HIS3* gene was included for selection of transformants in yeast. (**c**) Relative activity after induction of the reporter strain transformed with the indicated mutant vectors at three different temperatures compared to the wild type. In the leftmost lane (–), the reporter strain was transformed with an expression vector lacking a zinc-finger protein domain. (**d**) ZFN expression was monitored by western blot with an antibody to Flag (anti-Flag). Blots with antibody to histone H3 (anti-H3) were used as controls for loading.

double-strand break resulted in restoration of reporter gene expression (*MEL1* or *PHO5*) and simultaneous elimination of all positive and negative selection markers (**Fig. 1a**). We randomly mutagenized the sequence encoding the FokI nuclease domain using error-prone PCR and constructed a library of mutants *in vivo* by gap repair[18] (**Fig. 1b**). We induced ZFN expression at 22 °C (nonpermissive temperature), then collected the cells and incubated them in medium containing geneticin (G418) and nourseothricin to eliminate all cells carrying active ZFN constructs. Next, we shifted the cells to 37 °C (permissive temperature) and plated them on medium containing 5-fluoroorotic acid and a colorimetric substrate for the secreted acid phosphatase, Pho5, to select for conditionally active ZFNs (**Supplementary Fig. 1**). We confirmed the cold-sensitive phenotype of the isolated constructs by testing their activity at 22 °C, 30 °C and 37 °C; 16 mutants had background activity at 22 °C (<10% of wild-type activity) but had restored reporter gene expression at higher temperatures (**Fig. 1c**). All mutants expressed to similar levels, indicating that the variations in activity observed at the permissive temperature reflected the relative strength of the hypomorphic alleles (**Fig. 1d**).

In agreement with the hypothesis that cold-sensitive mutants would affect critical residues involved in dimerization, the mutated residues cluster at the dimer interface as judged from the FokI crystal structure[19] (**Fig. 2a**,**b**). We isolated mutations affecting three of the four residues previously altered by structure-guided engineering to obtain the first generation of FokI obligate heterodimeric variants, namely Ile499, Ile538 and Gln486 (ref. 6) (**Supplementary Table 1**). These data demonstrate that the cold-sensitivity screen identified both new and known residues critical for dimer formation.

Design of new engineered FokI cleavage half-domains

We focused on two residues, Asn496 and His537, that face each other in the FokI dimerization interface (**Fig. 2a**,**b**). These residues are located in (or directly adjacent to) a hydrophobic pocket disrupted during the engineering of the first-generation FokI obligate heterodimer variants, an alteration known to weaken dimerization[6,7,19]. Our molecular modeling studies suggested that substituting these residues with a pair of oppositely charged amino acids could favor the formation

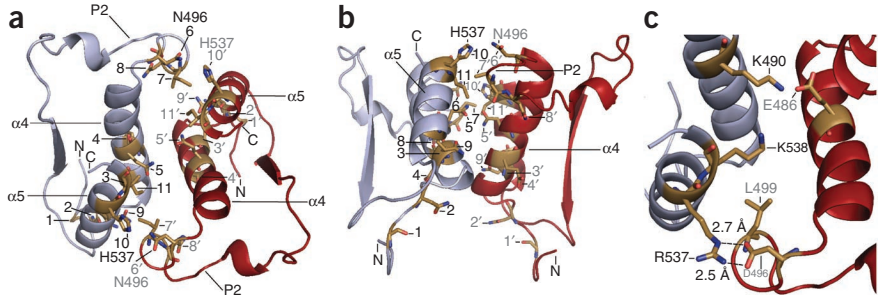

Figure 2 | Isolated mutations cluster to the FokI dimer interface. (**a**) Location of the mutations in the three-dimensional structure of the wild-type FokI dimer[19] interface amino acids 470–540. Mutated residues are shown in gold with oxygen atoms in red and nitrogen atoms in blue, and numbers refer to the mutations described in **Supplementary Table 1**. (**b**) Alternative representation of the dimer interface corresponding to an approximate 100° turn around the *x* axis. (**c**) Molecular modeling of the putative salt-bridge interaction between Arg537 and Asp496 in the obligate heterodimeric interface.

Table 1 | Engineered cleavage domain nomenclature

Cleavage domain	Mutations	Reference
EL	Q486E,I499L	6
EA	Q486E,I499A	7
ELD	Q486E,I499L,N496D	This work
ELE	Q486E,I499L,N496E	This work
REL	H537R,Q486E,I499L	This work
D[a]	R487D	7
DD[b]	R487D,N496D	This work
DA	R487D,I499A	7
DAD	R487D,I499A,N496D	This work
KK	E490K,I538K	6
KV	E490K,I538V	7
KKK	E490K,I538K,H537K	This work
KKR	E490K,I538K,H537R	This work
DKK	N496D,E490K,I538K	This work
R[a]	D483R	7
RR[b]	D483R,H537R	This work
RV	D483R,I538V	7
RVR	D483R,I538V,H537R	This work

[a]These mutants are also known as DD:RR (ref. 7) and 0 (ref. 10). To better represent the fact that they are single mutants and to maintain consistency with our nomenclature, we used a single letter to denote the parental mutants. [b]DD and RR are double mutants based on the parental R and D mutants, respectively.

of salt bridges[20] and thus strengthen dimerization in the context of the obligate heterodimer variants (**Fig. 2c**).

To test this hypothesis, we introduced pairs of amino acids carrying opposite charges into the EL:KK FokI obligate heterodimer backbone[6] (EL:KK denotes Q486E,I499L and E490K,I538K mutations). To preserve the anti-homodimerization behavior, we engineered the negatively charged N496D and N496E mutations into the EL domain, whereas we made the positively charged H537K and H537R substitutions to its KK counterpart, thus retaining all like charges in a given monomer. We refer to the new domains as ELD:KKK or ELD:KKR, that is, EL with N496D and KK with H537K or H537R mutations (**Table 1**).

We introduced these new FokI domains into a pair of ZFNs targeting *TP53BP1* and measured cleavage activity via the Surveyor Nuclease (Cel-1) assay[6,17,21] which determines the frequency of the small insertions and deletions (indels) characteristic of imprecise double-strand break repair by nonhomologous end-joining. As controls, we compared these domains to both wild-type and EL:KK versions. We observed a stable and reproducible 1.5–2-fold increase in Cel-1 signal compared to that for EL:KK-carrying ZFNs (**Supplementary Fig. 2**). These studies revealed that Asp496 drove maximal activity in the EL monomer (relative to Glu496), whereas substitution of a lysine or an arginine residue at position 537 resulted in similar activity improvements. Thus, we focused on comparisons of these three new variants.

To confirm the improved activity of our new FokI domains, we introduced them into a second pair of ZFNs targeting human *KDR*[22]. We observed a threefold reduction in cleavage activity with the EL:KK variants versus the wild-type FokI domain (**Fig. 3a**). Cleavage activity was fully rescued in the ELD:KKK and ELD:KKR variants, with the extent of gene disruption remaining stable through day 20 after transfection. All variants were expressed at similar levels as measured by western blot (**Fig. 3b**). We observed this increase in activity for seven different ZFN pairs, each targeting a unique site in the human genome, demonstrating the generality of this improvement both with respect to ZFN and DNA target site (**Supplementary Fig. 3**).

Next, we compared the activity of the different FokI domains using a highly active ZFN pair targeting the human glucocorticoid receptor (*NR3C1*) gene. In accordance with previous observations[6], use of optimized zinc-finger protein DNA-binding domain greatly reduced any loss of activity when we substituted the EL:KK mutant for the wild-type domains. The *NR3C1*-specific ZFN pair only revealed a reduction in cleavage activity in combination with the EL:KK mutations when ZFN dose was limiting (**Fig. 3c**). The new ZFN architectures outperformed EL:KK under these conditions, with the ELD:KKR combination resulting in the highest activity (**Fig. 3c**). We also explored whether the rates of ZFN-induced homologous recombination could be enhanced using a homology-directed repair assay[9]. We compared the ability of the EL:KK and ELD:KKR ZFNs to stimulate the targeting of a short stretch of exogenous DNA containing a BamHI restriction site (RFLP knock-in) at the *NR3C1* locus (**Fig. 3d**). We observed a 2.5-fold increase in homology-directed gene targeting that paralleled in magnitude the increase observed in gene disruption levels via nonhomologous end-joining.

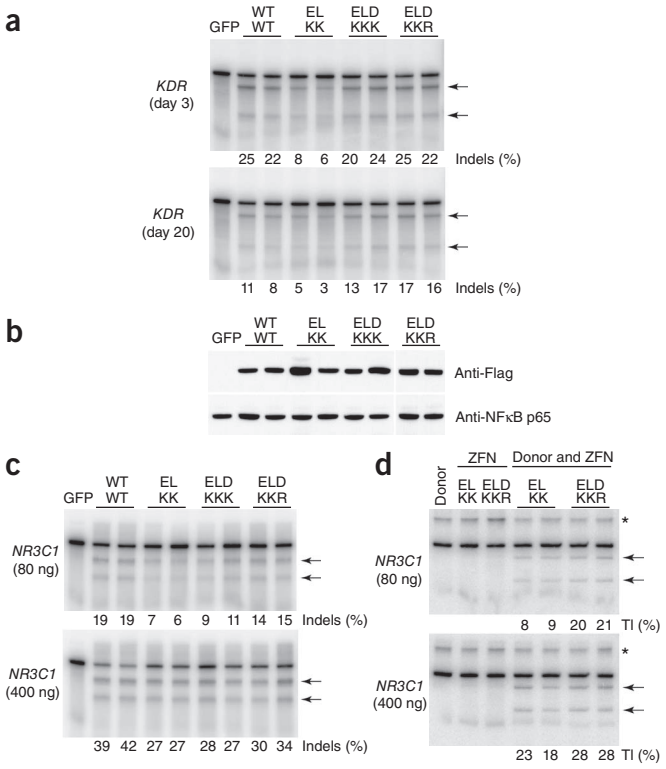

Figure 3 | Enhanced activity of the ELD:KKK and ELD:KKR architecture. (**a**) Autoradiograms showing results of a Cel-1 assay[6,17,21] to determine the frequency of ZFN-induced indels, conducted on genomic DNA from K562 cells collected 3 and 20 d after transfection with the indicated *KDR* ZFN constructs (400 ng). (**b**) Western blots showing ZFN expression. The NFκB p65 antibody was used as a loading control. (**c**) Autoradiograms showing results of a Cel-1 assay to determine the frequency of ZFN-induced indels, conducted on genomic DNA from K562 cells collected 3 d after transfection with the indicated *NR3C1* ZFN constructs (80 and 400 ng). (**d**) Autoradiograms showing results of a PCR-based assay[9] to determine ZFN-driven tag integration frequency, conducted on genomic DNA from K562 cells collected 3 d after transfection with the indicated *NR3C1* ZFN constructs (80 and 400 ng). The percentage of BamHI-sensitive DNA resulting from targeted integration (TI) of the donor is indicated below each lane. Arrows denote specific cleavage products. Asterisks indicate a nonspecific amplification product present in each lane. WT, wild type.

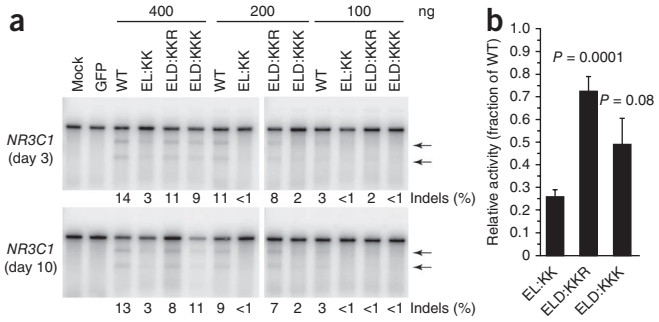

Figure 4 | Improved activity of new ZFN mutants in primary cells. (**a**) Autoradiograms showing results of a Cel-1 assay to determine the frequency of ZFN-induced indels, conducted on genomic DNA from PBMCs collected 3 d and 10 d after transfection with the indicated *NR3C1* ZFN constructs (100 ng, 200 ng and 400 ng). Arrows denote specific cleavage products. (**b**) Mean values (± s.e.m.) of the relative activities of the indicated ZFNs from six independent transfections into PBMCs as determined by Cel-1 assays conducted on genomic DNA collected at day 3 after transfection and using 400 ng of ZFN expression vector. *P* values were calculated using the two-sample *t*-test.

Enhanced activity in primary cells

A key motivation for improved ZFN architectures is to facilitate efficient genome engineering in cells and organisms that are both hard to transfect, that is, express low amounts of ZFN and require exquisite specificity. We therefore tested the effect of the new heterodimeric mutants in human peripheral blood mononuclear cells (PBMCs) using the *NR3C1* ZFNs. The ELD:KKR variants rescued ZFN activity to ~75% percent of the wild-type domain in these cells, a significant ($P = 0.0001$) improvement over the EL:KK architecture that yielded 25% gene disruption under optimized conditions (**Fig. 4**). Moreover, although the use of EL:KK domains did not yield any detectable signal when ZFN amounts were limiting, the ELD:KKR architecture drove strong gene modification. These results demonstrate the portability of the new FokI domain improvements across cells types, including those for which delivery and expression of the ZFN constructs are limiting.

Preservation of ZFN specificity

Strengthening the dimerization interface may, in principle, impair the obligate heterodimerization activity of the original FokI variants. To test the new domains, we used the *NR3C1* ZFNs and carried out three different specificity assessments. First, we evaluated the genome-wide DNA damage response at the whole-cell level by flow cytometry using a γ-H2AX marker (a molecular signature of double-strand breaks). As previously observed, use of the original obligate heterodimer ZFNs led to a marked decrease in the fraction of γ-H2AX antibody-stained cells[6,7], and the new FokI domains behaved indistinguishably compared to them (**Fig. 5a**).

Second, we assayed the same cell populations directly for gene disruption at the intended target site and at two homodimer off-target sites. The extent of *NR3C1* disruption obtained with the new FokI domains approached that of the wild type, with the ELD:KKR combination outperforming the ELD:KKK architecture (**Fig. 5b**). Thus, the markedly reduced DNA damage response cannot be explained by a simple reduction in overall ZFN activity. Next, we assayed two loci, *RCSD1* and *SREBF2*, that represent homodimer off-target sites for the *NR3C1* ZFNs. We detected no disruption at these sites using any of the obligate heterodimer ZFN variants, but gene disruption was evident when using the wild-type version (**Fig. 5b**). These differences in activity were not caused by changes in ZFN expression, as gauged by western blot (**Fig. 5c**).

Third, to more stringently test dimerization potential, we measured the interaction of identical domains via forced homodimerization at the intended *NR3C1* target site. This artificial context (placing the identical FokI variant on each of two-custom engineered zinc-finger protein DNA-binding domains for a given target site) was intended to maximize the potential for ZFN-induced cleavage owing to homodimerization. Despite observing indels in >40% of the *NR3C1* alleles using the wild-type domain,

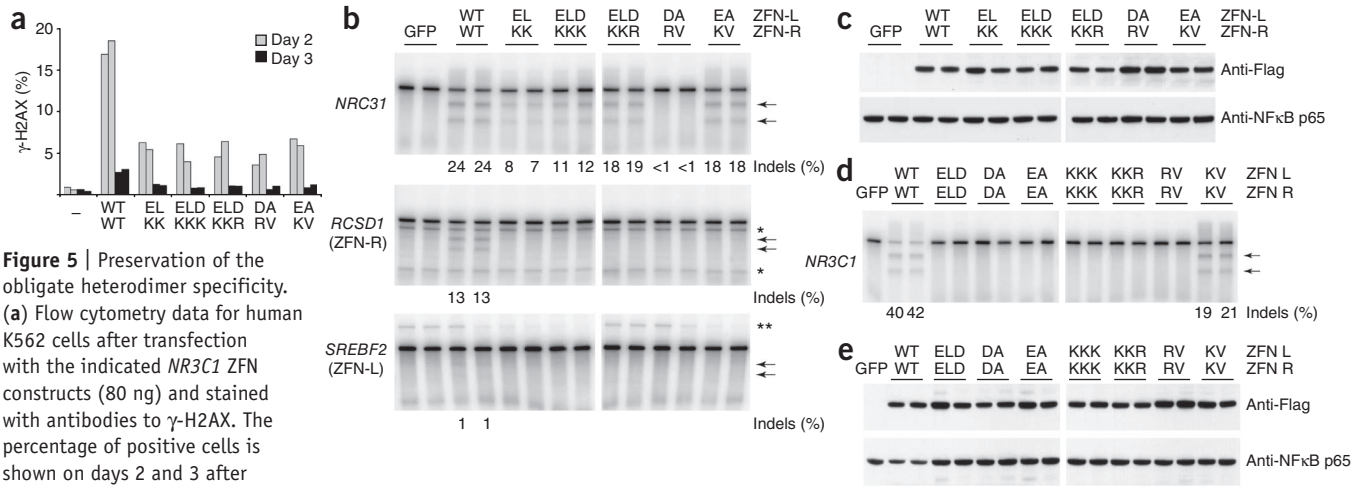

Figure 5 | Preservation of the obligate heterodimer specificity. (**a**) Flow cytometry data for human K562 cells after transfection with the indicated *NR3C1* ZFN constructs (80 ng) and stained with antibodies to γ-H2AX. The percentage of positive cells is shown on days 2 and 3 after transfection. Data from two independent transfections are shown. (**b**) Autoradiograms showing results of a Cel-1 assay to determine the frequency of ZFN-induced indels at the intended target (*NR3C1*) and two homodimer off-target sites, found in noncoding regions of *RCSD1* and *SREBF2* genes, conducted on genomic DNA from K562 cells collected 3 d after transfection. Arrows denote specific cleavage products. *, nonspecific cutting by the Cel-1 nuclease. **, nonspecific amplification product present in each lane. (**c**) Western blots showing ZFN expression. The NFκB p65 antibody was used as a loading control. (**d**) Autoradiograms showing results of a Cel-1 assay to determine the frequency of ZFN-induced indels, conducted on genomic DNA from K562 cells collected 3 d after transfection with the indicated *NR3C1* ZFN constructs (400 ng). Arrows denote specific cleavage products. (**e**) ZFN expression monitored as in **c**.

we could not detect activity (assay sensitivity ~1%) with any combination of FokI variants (**Fig. 5d** and **Supplementary Fig. 4**). Whole-cell extracts from transfected cells showed that all variants were expressed at similar levels (**Fig. 5e**). As suggested by the γ-H2AX marker, strengthening the heterodimer interface did not result in promiscuous cleavage at heterodimeric off-target sites (**Supplementary Fig. 5**).

To confirm that the restriction on productive homodimerization was neither ZFN-dependent nor target sequence–dependent, we assessed forced homodimerization using the *CCR5*-specific ZFNs[17,23]. Again, we could not detect ZFN-induced indels at off-target homodimer sites when using obligate heterodimeric FokI domains (**Supplementary Figs. 6** and **7**). However, ZFN overexpression coupled with forced homodimerization at the *CCR5* locus revealed low activity cleavage for the EL variants. Notably, use of the N496D mutation (ELD domain) reduced the observed frequency of indels by approximately twofold (**Supplementary Fig. 7**). Taken together, these data demonstrate that the ELD:KKR variants retained (and in one case improved) obligate heterodimer specificity and had enhanced on-target activity relative to the EL:KK parental architecture.

Portability of the new FokI mutations

Two sets of obligate heterodimer mutations have been previously described[6,7] (**Table 1**). Having demonstrated the improvements possible with the EL:KK backbone, we next tested whether similar improvements in cleavage activity could be obtained in the context of the EA:KV (EA:KV denotes Q486E,I499A and E490K,I538V mutations) and DA:RV (DA:RV denotes R487D,I499A and D483R,I538V mutations) domains[7] (**Table 1**). Evaluation of EA:KV provided an initially impressive on-target cleavage activity but revealed weak anti-homodimerization activity, and we did not analyze these mutations subsequently (**Fig. 5d**). We observed markedly reduced cleavage activity when we tested the DA:RV mutants in combination with either the *NR3C1*- or *CCR5*-specific ZFNs (**Fig. 5b** and **Supplementary Fig. 6**) in accordance with recent data highlighting the severely attenuated activity of these domains[10]. Remarkably, addition of the N496D and H537R mutations to generate the DAD:RVR domains (**Table 1**) revealed a two- to threefold improvement in activity in the context of the *NR3C1*, *CCR5* and *CXCR4* ZFNs (**Supplementary Fig. 8**). We observed similar improvements for the DD:RR versions of the single-mutant D:R parental domains[7] (**Table 1** and **Supplementary Fig. 9**). Together these data demonstrate that our N496D and H537R mutations improved activity independently of the mutations used to prevent homodimerization.

Generation of enhanced orthogonal ZFN pairs

For certain applications it would be highly desirable to have two sets of mutually independent ZFN pairs, for example, when targeting two genomic loci simultaneously[10]. To this end we evaluated the cleavage activity of the DAD:RVR and ELD:KKR variants as (i) the intended heterodimers and (ii) as all possible permutations of homodimers and *trans*-heterodimers, that is, across pairs. These data demonstrate that although each intended ZFN pair (DAD:RVR and ELD:KKR) was highly active, both homodimer and trans-heterodimer formation was eliminated or reduced by at least tenfold (**Supplementary Fig. 10**). To demonstrate the potential of these orthogonal ZFN pairs, we simultaneously targeted the *CCR5* (refs. 17,23) and *CXCR4* (ref. 24) genes, the two major HIV co-receptors, using a combination of the ELD:KKR (*CCR5*) and DAD:RVR (*CXCR4*) FokI domains. Although we observed mutation frequencies exceeding 50% at both intended targets, we did not detect any cleavage at trans-heterodimer off-target sites (**Supplementary Fig. 11**). The extent of mutual independence of the two ZFN sets was highlighted by the data for the *TBC1D5* off-target. At this *trans*-heterodimerization off-target, we observed a drop from 40% gene disruption when dimerization was permitted, down to undetectable levels with the orthogonal domains (**Supplementary Fig. 11**). These data demonstrate that the introduction of the N496D and H537R mutations resulted in a robust improvement of ZFN activity and preserved the incompatibility between the DA:RV and EL:KK domains necessary for orthogonal ZFN pair behavior.

DISCUSSION

Although we expected that the ELD:KKR domains would be broadly portable to alternative zinc-finger protein DNA-binding domains, we also found that the N496D and H537R mutations resulted in enhanced ZFN activity in the context of all published obligate heterodimeric FokI domains including the recently described high-activity FokI nuclease domain referred to as Sharkey[25]. Using ZFNs targeting two endogenous genes, we observed a similar improvement in activity with either Sharkey or the ELD:KKR domains alone (**Supplementary Figs. 12** and **13**). Combining Sharkey and ELD:KKR mutations resulted in an additive effect on ZFN activity, suggesting that they act by different mechanisms (**Supplementary Figs. 12–14**). In addition, the improvements observed with the ELD:KKR domains were also additive with the previously reported 'cold-shock' treatment[22], demonstrating their broad capacity to improve ZFN action (**Supplementary Fig. 3b**).

The ELD:KKR variants offer unique advantages as compared to general techniques used for enhancing ZFN action, such as improved delivery methods or the cold shock. First, in addition to increased ZFN cleavage activity, the ELD:KKR mutants restrict residual homodimerization, which increases genome 'safety'. Second, the portability to any zinc-finger protein or FokI architecture means that these improvements in activity and specificity can be realized even in systems that may in practice be resistant to a 'cold shock', for example, in plants or *in vivo*. Third, the new mutants drive an increase in ZFN-stimulated homologous recombination, a result that has proven elusive with the 'cold-shock' method alone.

Finally, the cold-sensitive mutants described here potentially offer conditional control over ZFN activity. These mutants might be used in the development of cell lines or whole organisms, such as plants, in which cleavage activity would be induced by transiently raising the ambient temperature. The use of these variants would provide a simple, efficient and autonomous way to activate or repress ZFN action in physiological conditions without relying on small molecules to achieve regulation.

METHODS

Methods and any associated references are available in the online version of the paper at http://www.nature.com/naturemethods/.

Note: Supplementary information is available on the Nature Methods website.

ACKNOWLEDGMENTS

We thank A. Reik for providing critical reagents and assistance with the manuscript, S. Abrahamson for careful reading of the manuscript and E. Lanphier for encouragement and support.

AUTHOR CONTRIBUTIONS

Y.D. and S.G.G. isolated the cold-sensitive mutants. Y.D., T.D.V., M.C.M., J.W. and D.F.X. characterized the engineered domains. Y.D., J.C.M. and M.C.H. designed the experiments. Y.D., F.D.U., P.D.G. and M.C.H. wrote the manuscript.

COMPETING FINANCIAL INTERESTS

The authors declare competing financial interests: details accompany the full-text HTML version of the paper at http://www.nature.com/naturemethods/.

Published online at http://www.nature.com/naturemethods/.
Reprints and permissions information is available online at http://npg.nature.com/reprintsandpermissions/.

1. Kim, Y.G., Cha, J. & Chandrasegaran, S. Hybrid restriction enzymes: zinc finger fusions to Fok I cleavage domain. *Proc. Natl. Acad. Sci. USA* **93**, 1156–1160 (1996).
2. Klug, A. The discovery of zinc fingers and their applications in gene regulation and genome manipulation. *Annu. Rev. Biochem.* **79**, 213–231 (2010).
3. Carroll, D. Progress and prospects: zinc-finger nucleases as gene therapy agents. *Gene Ther.* **15**, 1463–1468 (2008).
4. Urnov, F.D., Rebar, E.J., Holmes, M.C., Zhang, H.S. & Gregory, P.D. Genome editing with engineered zinc finger nucleases. *Nat. Rev. Genet.* **11**, 636–646 (2010).
5. Kim, J.S., Lee, H.J. & Carroll, D. Genome editing with modularly assembled zinc-finger nucleases. *Nat. Methods* **7**, 91 (author reply, 91–92) (2010).
6. Miller, J.C. *et al.* An improved zinc-finger nuclease architecture for highly specific genome editing. *Nat. Biotechnol.* **25**, 778–785 (2007).
7. Szczepek, M. *et al.* Structure-based redesign of the dimerization interface reduces the toxicity of zinc-finger nucleases. *Nat. Biotechnol.* **25**, 786–793 (2007).
8. Handel, E.M., Alwin, S. & Cathomen, T. Expanding or restricting the target site repertoire of zinc-finger nucleases: the inter-domain linker as a major determinant of target site selectivity. *Mol. Ther.* **17**, 104–111 (2009).
9. Urnov, F.D. *et al.* Highly efficient endogenous human gene correction using designed zinc-finger nucleases. *Nature* **435**, 646–651 (2005).
10. Sollu, C. *et al.* Autonomous zinc-finger nuclease pairs for targeted chromosomal deletion. *Nucleic Acids Res.* advance online publication 16 August 2010 (doi:10.1093/nar/gkq720).
11. Bitinaite, J., Wah, D.A., Aggarwal, A.K. & Schildkraut, I. FokI dimerization is required for DNA cleavage. *Proc. Natl. Acad. Sci. USA* **95**, 10570–10575 (1998).
12. Cai, C.Q. *et al.* Targeted transgene integration in plant cells using designed zinc finger nucleases. *Plant Mol. Biol.* **69**, 699–709 (2009).
13. Doyon, Y. *et al.* Heritable targeted gene disruption in zebrafish using designed zinc-finger nucleases. *Nat. Biotechnol.* **26**, 702–708 (2008).
14. Geurts, A.M. *et al.* Knockout rats via embryo microinjection of zinc-finger nucleases. *Science* **325**, 433 (2009).
15. Shukla, V.K. *et al.* Precise genome modification in the crop species *Zea mays* using zinc-finger nucleases. *Nature* **459**, 437–441 (2009).
16. Hampsey, M. A review of phenotypes in *Saccharomyces cerevisiae*. *Yeast* **13**, 1099–1133 (1997).
17. Perez, E.E. *et al.* Establishment of HIV-1 resistance in CD4+ T cells by genome editing using zinc-finger nucleases. *Nat. Biotechnol.* **26**, 808–816 (2008).
18. Muhlrad, D., Hunter, R. & Parker, R. A rapid method for localized mutagenesis of yeast genes. *Yeast* **8**, 79–82 (1992).
19. Wah, D.A., Bitinaite, J., Schildkraut, I. & Aggarwal, A.K. Structure of FokI has implications for DNA cleavage. *Proc. Natl. Acad. Sci. USA* **95**, 10564–10569 (1998).
20. Kumar, S. & Nussinov, R. Close-range electrostatic interactions in proteins. *ChemBioChem* **3**, 604–617 (2002).
21. Guschin, D.Y. *et al.* A rapid and general assay for monitoring endogenous gene modification. *Methods Mol. Biol.* **649**, 247–256 (2010).
22. Doyon, Y. *et al.* Transient cold shock enhances zinc-finger nuclease-mediated gene disruption. *Nat. Methods* **7**, 459–460 (2010).
23. Holt, N. *et al.* Human hematopoietic stem/progenitor cells modified by zinc-finger nucleases targeted to CCR5 control HIV-1 *in vivo*. *Nat. Biotechnol.* **28**, 839–847 (2010).
24. Del Prete, G.Q. *et al.* Derivation and characterization of a simian immunodeficiency virus SIVmac239 variant with tropism for CXCR4. *J. Virol.* **83**, 9911–9922 (2009).
25. Guo, J., Gaj, T. & Barbas, C.F., III. Directed evolution of an enhanced and highly efficient FokI cleavage domain for zinc finger nucleases. *J. Mol. Biol.* **400**, 96–107 (2010).

ONLINE METHODS

Yeast reporter strain. To modify the *MEL1* single-strand annealing (SSA) reporter[13], a BglII fragment from pFL38 (American Type Culture Collection (ATCC) 77203) containing the *URA3* gene was cloned into the BglII site of the vector. Next, the *CCR5-L* homodimer site was introduced by annealing and ligation of the following oligos: 5′-gatccggtcatcctcatcctgaggatgaggatgacct tttgcagtttatgataaactgcaaaaggg-3′and 5′-cgcgccctttgcagtttatcataa actgcaaaaggtcatcctcatcctcaggatgaggatgaccg-3′ into the BamHI and BssHII sites. The *PHO5* SSA reporter had the same basic structure and was assembled by successive modification of the *MEL1* SSA reporter[13], but it was targeted to the endogenous *PHO5* locus in the yeast genome. First, a fragment corresponding to nucleotides 1–750 of the *PHO5* gene (relative to the ATG codon) was cloned into the SalI and BamHI sites using the primers 5′–atatctcgagatgtttaaatctgttgtttattc-3′ and 5′-atatggatccg ttcaaacccttgttttccttgttc-3′. Then, a fragment from nucleotides 299 to the poly(A) sequence was cloned into the SacI and EcoRI sites using the following primers: 5′-atatgagctcgtcaattcaacggctcattgtc-3′ and 5′–atatgaattcaggtaatttggaatggccctttc-3′. The *kanMX* ORF was then exchanged for the *natMX* ORF by cloning a NcoI-SacI fragment from pAG25 (Euroscarf DEL-MARKER-SET). To eliminate the HO-R targeting arm, the construct was cut with EcoRI and SfiI, blunted and religated. To eliminate the HO-L targeting arm, the construct was cut with BsgI and NotI, blunted and religated. Finally, the *CCR5-L* homodimer site was introduced by cloning a BamHI-NcoI fragment from the corresponding *MEL1* SSA reporter. The yeast reporter strain was constructed by sequential integration of the two reporter constructs in the BY4741 background using standard procedures[13]. Note that the *PHO5* SSA reporter needs to be linearized using the SpeI enzyme before integration.

Random mutagenesis. The full-length wild-type FokI domain was mutagenized using the GeneMorph II Random Mutaganesis Kit (Stratagene) following manufacturer's recommendations. The following primers were used for the amplification: *CYC1t* gap repair 5′-ttgtctaactccttccttttcggttagagcggatgtgggagga gggcgtgaatgtaagcgtgacataactaattacatgatatcg-3′ and *CCR5-L* gap repair 5′–cgagaagccttttgcctgtgacatttgtgggaggaagtttgccacctcc ggcaacctgacccgccataccaagatacacctgcgg-3′. Three libraries with mutation frequency of low (0–4.5 mutations per kb), medium (4.5–9 mutations per kb) and high (9–16 mutations per kb) range were used to transform the yeast reporter strain. Each of these libraries were transformed and screened independently. Because we selected transformed cells in liquid media we cannot determine precisely the size of the mutant's library. However, based on preliminary testing of the gap repair efficiency on solid medium, we estimated that the size of the combined libraries approached 10^5.

Gap repair and screen. The yeast expression vector encoding the *CCR5-L* ZFN has been described previously[13] and was linearized with BamHI and XhoI before transformation. The reporter strain was transformed at an approximately 10:1 insert: vector molar ratio, and selection for transformed cells was done for 3 d in liquid synthetic drop-out medium lacking histidine at 22 °C. Note that yeast nitrogen base without ammonium sulfate and supplemented with 1 g l^{-1} of glutamate was used because G418 and NAT are not active otherwise. The cells were then centrifuged and resuspended in raffinose medium lacking histidine at 22 °C overnight. ZFN expression was induced by adding 2% galactose to the cultures for six hours and stopped by addition of 2% glucose. The next day, cells were transferred to glucose medium lacking histidine and uracil and supplemented with 200 µg ml^{-1} G418 and 100 µg ml^{-1} NAT and kept at 22 °C for 2 d. The cells where then washed once with water, resuspended in glucose medium lacking histidine and incubated at 37 °C for 3 d as an attempt to isolate the most active mutants during the next step of selection. We observed that the low levels of wild-type *CCR5-L* ZFNs resulting from the basal expression of the *GAL1* promoter in glucose medium allowed cleavage of the reporter in a fraction of the cells. Thus, we reasoned that incubating cells at the permissive temperature in absence of galactose induction should favor the isolation of the most active mutants from the cultures. Finally, the cells were plated on glucose medium without histidine supplemented with 0.1% 5-fluoroorotic acid (5-FOA; Biosynth) and 40 mg l^{-1} 5-bromo-4-chloro-3-indoxyl phosphate (X-Phos; Biosynth) at 37 °C for 3 d. We isolated plasmids from 61 'blue' colonies and tested the mutants for activity at 22 °C, 30 °C and 37 °C as described previously[13]. Of this set, 32 displayed a cold-sensitive phenotype. These mutants were enriched in the low and medium mutation frequency libraries.

Cell culture and transfection. K562 cells were obtained from the ATCC and maintained at 37 °C under 5% CO_2 in RPMI medium supplemented with 10% FBS. K562 cells were transfected using the 96-well Nucleofector Kit SF (Lonza) per manufacturer's recommendations. PBMCs (AllCells) were received on ice, centrifuged at 1,000*g* for 5 min at room temperature (22 °C) and changed to pre-warmed RPMI medium supplemented with L-glutamine, 10% FBS and 30 U ml^{-1} rhIL-2 (Roche). Cells were allowed to recover for 6–8 h before transfection using the 96-well Nucleofector Kit for human T cells (Lonza) according to the manufacturer's instructions. Sixteen to twenty hours after transfection, anti-CD3 and CD28 beads (Invitrogen) were added at a 1:1 ratio as per manufacturer's recommendations.

ZFN reagents. The full sequences of the *TP53BP1*, *NR3C1* and *CXCR4* ZFNs are listed in **Supplementary Note 1**. The *CCR5* ZFNs have been previously described[17]. The *KDR* and *RIPK1* ZFNs were obtained from Sigma-Aldrich. Site-directed mutagenesis of the FokI domain was performed using the QuikChange Lightning kit (Stratagene). All constructs were confirmed by sequencing. The primary amino acid sequences of the wild-type and obligate heterodimeric FokI mutants have been previously described[6,7].

Surveyor nuclease (Cel-1) assay. Genomic DNA was extracted from cells using the QuickExtract DNA Extraction Solution (Epicentre). ZFN target loci (~300 bp) were PCR-amplified (30 cycles, 60 °C annealing, 30 s elongation) using the primers described in **Supplementary Table 2**. The assays were carried out as described previously[6,17,21].

RFLP knock in assay. Genomic DNA was extracted from cells using the QuickExtract DNA Extraction Solution (Epicentre) 3 d after transfection. The *NR3C1* locus was amplified by 25 cycles of

PCR (1.5 min extension time at 68 °C and 30 s annealing at 62 °C) in the presence of radiolabeled dNTPs using the following primers: 5′-ataatcactagacctgcactctttgtggtg-3′ and 5′-cagttc tcactgtgactcatttttgcca-3′. The PCR products were then purified with G50 columns, digested with BamHI, resolved by 10% PAGE and autoradiographed. The donor plasmid was constructed by cloning an 805-bp fragment from the *NR3C1* locus surrounding the ZFN binding site into pCR4-TOPO (Invitrogen). A 38-bp tag sequence containing a BamHI restriction site was then introduced at the ZFN cut site by site directed mutagenesis. The sequence of the donor vector is available in **Supplementary Note 2**.

γ-H2AX staining. The percentage of γ-H2AX positive cells was determined by flow cytometry as described previously[6].

Statistical testing. *P* values were calculated using the two-sample *t*-test calculated by MicroCal Origin version 7.5.

Gels and blots. For all data shown in the paper, full-length gels and blots are presented in **Supplementary Figure 15**.

Western blot. One million cells were lysed directly in 100 µl of loading buffer by boiling. Antibodies to Flag M2 (Sigma; 1:1,000) and to NFκB p65 (Santa Cruz; 1:3,000) were used.

doi:10.1038/nmeth.1539